



Contents lists available at ScienceDirect

Nuclear Inst. and Methods in Physics Research, A

journal homepage: www.elsevier.com/locate/nima

Operation of a silicon microstrip detector prototype for ultra-fast imaging at a synchrotron radiation beam

L. Shekhtman^{a,d,*}, V. Aulchenko^a, D. Kudashkin^{a,d}, V. Kudryavtsev^{a,d}, E. Prueel^{c,d}, K. Ten^c,
B. Tolochko^{b,d}, V. Zhulanov^{a,d}

^a Budker Institute of Nuclear Physics, 630090, Novosibirsk, Russian Federation

^b Institute of Solid State chemistry and Mechanochemistry, 630090, Novosibirsk, Russian Federation

^c Lavrentyev Institute of Hydrodynamics, 630090, Novosibirsk, Russian Federation

^d Novosibirsk State University, 630090, Novosibirsk, Russian Federation

ARTICLE INFO

Keywords:

Time resolved studies

X-ray detectors

Synchrotron radiation

ABSTRACT

A method of imaging of ultra-fast processes, like explosions or fast combustion, at a synchrotron radiation beam is being developed at the Siberian Synchrotron and Terahertz Radiation Center (SSTRC). Two stations are equipped with the detector for imaging of explosions, DIMEX, based on high pressure ionization chamber, and allowing to record up to 100 one dimensional images with a frame rate of 8 MHz. However the maximum flux that DIMEX can detect is limited as well as the spatial resolution and the frame rate because of the gas technology used. In view of the significant increase of SR flux at the VEPP-4M beam line due to the new 9-pole 2 T wiggler, a new detector is being developed for this beam line, based on Si microstrip sensor. The first Si microstrip detector prototype has been mounted with a new specially developed front-end ASIC that allows to record data with a rate up to 40 MFrames/s. The first measurements with this prototype demonstrated significant improvement of all critical parameters of the detector compared to the gaseous version. The maximum detected photon rate before saturation is increased to 20000 photons/(channel x bunch) compared to 1500 photons/(channel x bunch). The spatial resolution is improved from 240 μm to 130 μm (FWHM) and the frame rate is increased by a factor 5.

1. Introduction

Experiments on imaging of fast dynamic processes (explosions, combustion) with a synchrotron radiation beam are performed in the Budker INP at the VEPP-3 storage ring for more than 15 years [1–4]. The DIMEX (Detector for IMaging of EXplosions) based on gas technology is used for this purpose [5–10]. DIMEX allows to measure a photon flux up to ~ 5000 photons/(channel \times bunch)(channel area is $0.1 \times 0.5 \text{ mm}^2$, average photon energy $\sim 20 \text{ keV}$), with a spatial resolution of $\sim 0.2 \text{ mm}$ and a frame rate of 10 MHz. In order to improve all detector parameters, namely, maximum measured photon flux up to 10^6 photons/(channel \times bunch), spatial resolution down to 50 μm and maximum frame rate up to 50 MHz, a new development was started based on Si microstrip technology [11,12]. A new beam line with ~ 100 times higher flux and higher X-ray energy is constructed for this purpose at the VEPP-4M storage ring [13].

A schematic view of the experimental set-up is shown in Fig. 1. The SR beam is provided by a 9-pole wiggler with 7 poles having 2 T field and the first and the last poles having 1.2 T field [14,15]. The beam passes through the collimator block forming a flat narrow beam,

the explosion chamber that can withstand an explosion of 200 g of trinitrotoluene (TNT) and then passes to the detector hutch.

The VEPP-4M storage ring operates at present with an electron beam energy up to 4.5 GeV and a beam current up to 20 mA (in two bunches). In future the energy will be increased to 5 GeV and the beam current will be increased to 20 mA in each bunch. The bunches can be grouped in trains of 4–5 bunches with 20 ns time gaps. The calculated energy spectrum at the entrance of the detector in comparison with the spectrum in the VEPP-3 beam line is shown in Fig. 2 [16]. Total integrated photon flux before the detector, taking into account the distance from the source and all the absorbers, is indicated in the figure for both beam lines.

A Si microstrip detector with a thin sensor aligned at a small angle with respect to the beam plane and with the strips parallel to the beam direction can provide the required improvement of the parameters. The limitation of the maximum rate in the gaseous detector is determined by ion space charge that affects the drift of electrons. Mobilities of electrons and holes in silicon are not so different as those of electrons and ions in gas and have much higher values. Thus, space charge

* Corresponding author at: Budker Institute of Nuclear Physics, 630090, Novosibirsk, Russian Federation.

E-mail address: L.I.Shekhtman@inp.nsk.su (L. Shekhtman).

<https://doi.org/10.1016/j.nima.2019.162655>

Received 21 March 2019; Received in revised form 23 August 2019; Accepted 30 August 2019

Available online xxx

0168-9002/© 2019 Elsevier B.V. All rights reserved.

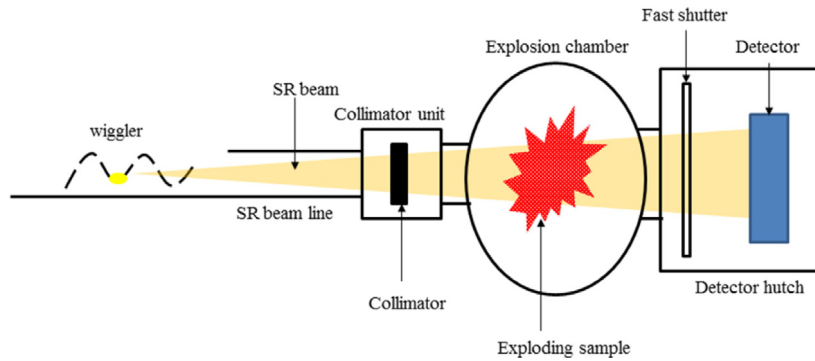


Fig. 1. Schematic view of the experiment for direct imaging of exploding sample.

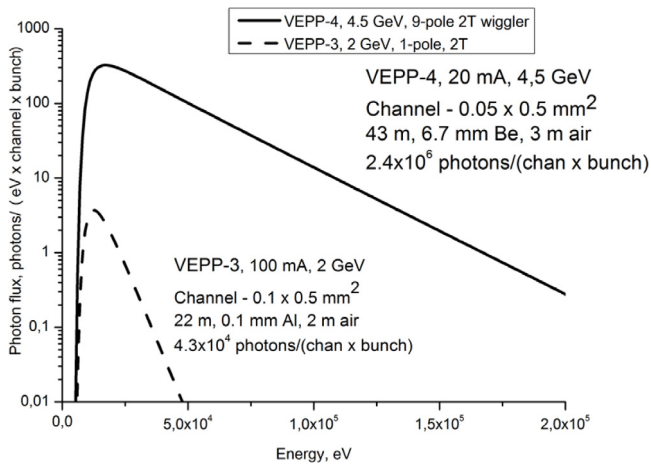


Fig. 2. Energy spectrum of the SR beam before the detector in the beam line 8 of the VEPP-4M storage ring in comparison with the spectrum in the VEPP-3 beam line 0.

effects in silicon start at much higher rates than in high pressure Xe. The charge collection time in a 0.3 mm thick Si sensor is about 100 times shorter than in a 1 mm thick high pressure Xe layer, therefore time resolution of Si detector will be much better. Finally, the spatial resolution of gaseous detector is determined by electron diffusion that is much higher than in Si.

2. Design of the silicon microstrip detector prototype

The prototype detector is based on a p-in-n, 320 μm thick sensor with strip implants at 50 μm pitch, DC-coupled to aluminium readout strips and with $\sim 400 \Omega$ polysilicon resistors connecting each strip to the guard ring. The sensor is $55 \times 35 \text{ mm}^2$ in size and contains 1024 30 mm long strips (Fig. 3). It was manufactured for us by the Hamamatsu Photonics company.

Each strip is connected to an input of the front-end ASIC through a 10 k Ω resistor in order to limit the current to the front-end ASIC. A dedicated ASIC was developed for this detector that allows to measure the signal at the resistor at each strip with 20 ns duty cycle. A block diagram of one channel of this ASIC is shown in Fig. 4. It contains voltage to current converter at the input that transfers voltage pulses at the input resistor to the current pulse at the output, a DC compensation circuit and a commutator to four integrators with reset circuit and analog memory. In order to provide the fastest operation, the integrators are switched to the output of the voltage to current converter by turns one at a time, because the reset circuit of the feedback capacitor cannot discharge it within 20 ns. The prototype ASIC was manufactured with 6 channels, each containing 4×8 analogue memory cells.

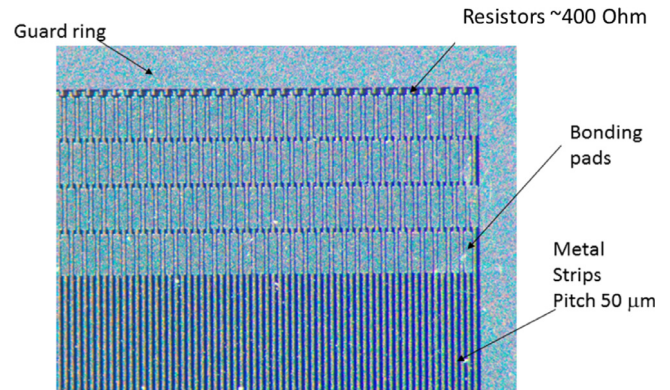


Fig. 3. Photograph of the Si sensor.

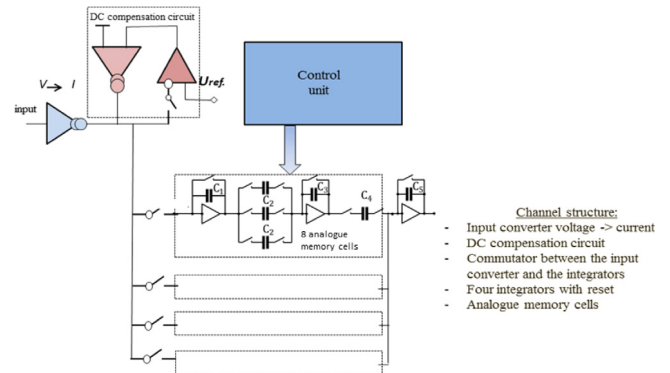


Fig. 4. Block-diagram of one channel of the DMXS6A ASIC for the Si microstrip detector for imaging of explosions.

The prototype, based on Si micro-strip sensor with 16 DMXS6A ASICs, was assembled and put into operation (see Figs. 5 and 6). It consists of the board for the sensor with 48 strips bonded to the connectors from each side. The sensor board is connected to two front-end boards each containing 8 DMXS6A chips. The output signal from each chip is digitized by a 14-bit 3 Msp/s ADC and then the digital data are transferred to the memory at the motherboard. The data are readout to a computer through a 1 Gbit Ethernet connection. The motherboard provides the trigger signal and all control sequences that allow proper operation of the ASICs and ADCs.

3. Results of the tests at a SR beams

The prototype detector was irradiated at the SR beam at channel 0 at the VEPP-3 storage ring and at channel 8 at the VEPP-4M storage

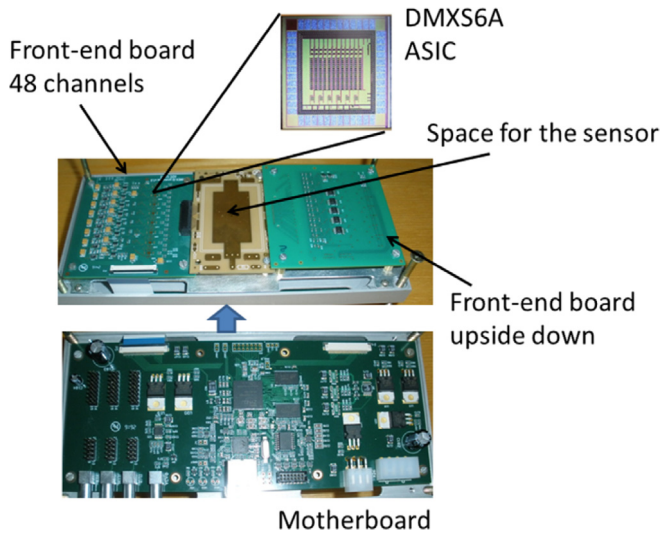


Fig. 5. Components and layout of the 96 channel prototype of the Si detector for imaging of explosions.

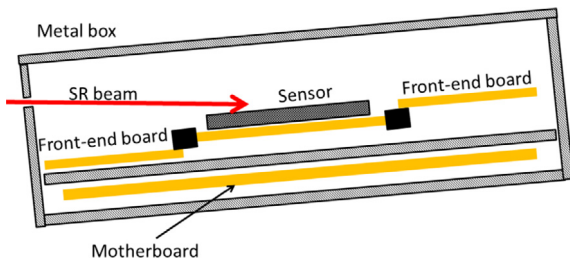


Fig. 6. Schematic view of the prototype of the DIMEX-Si installed at the SR beam.

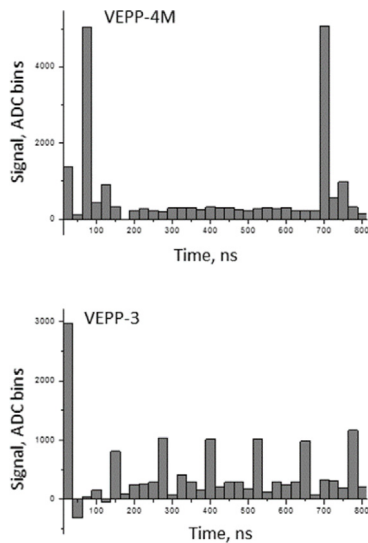


Fig. 7. Signal from a single channel as a function of time. Top: irradiation at the VEPP-4M, 625 ns between bunches; bottom: irradiation at the VEPP-3, 125 ns between bunches.

ring. The detector operation cycle includes the exposure phase, when voltage at the input is transferred to current that is integrated at the feedback capacitance of the integrator. At the end of this phase the feedback capacitor is coupled to an analogue memory cell and then the feedback capacitor is discharged by the reset switch. The dependence of the signal on time for one channel of the detector is shown in Fig. 7.

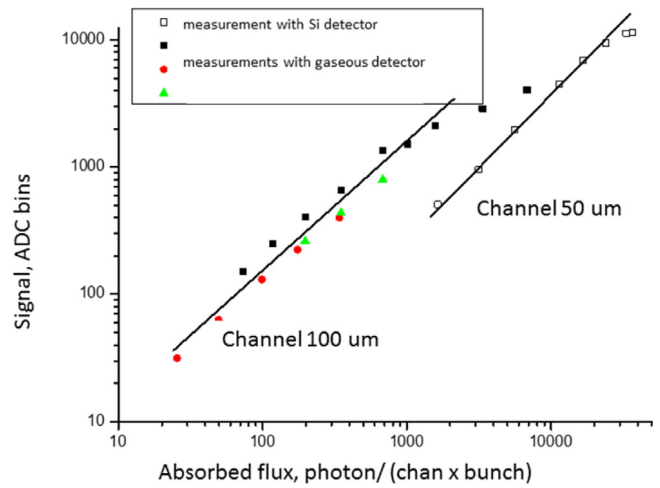


Fig. 8. Signal as a function of absorbed flux per channel per bunch. Comparison of gaseous and silicon detectors.

The detector was operated with a 25 ns cycle during these measurements. Fig. 7 demonstrates that the signal is recorded within one cycle of the detector operation and signals from single bunches are well separated from each other.

By irradiating the detector uniformly and changing the SR flux per detector channel by changing the beam height, the detector signal as a function of SR flux dependence was measured. The absorbed SR flux was calculated using the XOP program [16]. A comparison of such dependences for the present prototype and the gaseous version of the DIMEX are shown in Fig. 8.

A non-linear dependence of the signal on the SR flux for the gaseous detector starts approximately at an absorbed flux of 1500 photons/(chan \times bunch) (channel width is 100 μm), while for the silicon detector the limit of linearity is measured at $\sim 20\,000$ photons/(chan \times bunch) for 50 μm wide channel. Thus we can see that the silicon prototype demonstrated 30 times higher rate capability as compared to the gaseous DIMEX. Moreover, for the gaseous detector the rate limiting factor is space charge effect, while for the Si prototype the rate is limited due to saturation of the integrators of the front-end ASIC. By changing the current divider at the input of the front-end chips one can tune the rate limit of the detector. However this measurement demonstrated significant noise of the DMXS6A ASIC, that did not allow to get reliable results at an absorbed flux below ~ 1000 photons/(chan \times bunch). The reasons of this noise are under careful investigation now.

The spatial resolution of the detector prototype was measured using the method of opaque edge. A 3 mm thick steel plate with a well defined edge was attached to the detector inlet window perpendicular to the beam plane. An image of the edge was fitted with a smooth function and the derivative of this function is the line spread function, a measure of spatial resolution. A comparison of the line spread functions of the gaseous and silicon detectors obtained by such method are shown in Fig. 9. Full width at half maximum of the line spread function of the silicon detector is equal to 130 μm that is almost twice better than that of the gaseous detector.

4. Conclusions

The first measurements of the main parameters of the silicon detector prototype at a synchrotron radiation beams demonstrated significant improvements in all aspects as compared to the gaseous version of the DIMEX. The time resolution of the new detector is well below 25 ns, the signal is recorded within one detector cycle and signals from single bunches are well separated from each other. Thus, operation with frame rate of 40 MHz was demonstrated. The maximum detected photon

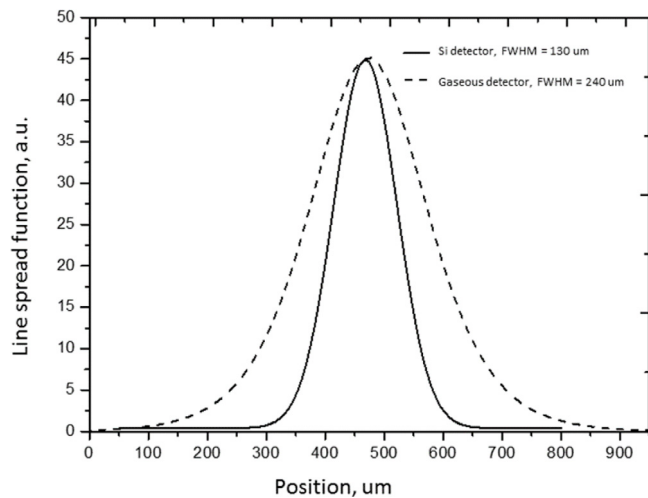


Fig. 9. Line spread functions calculated from the fits to the images of the opaque edge. Comparison of the gaseous and silicon detectors.

rate before saturation is increased to 20 000 photons/(chan × bunch) compared to 1500 photons/(chan × bunch) for the gaseous detector. The spatial resolution is improved from 240 μm to 130 μm. The problem of high noise of the new front-end ASIC is under investigation, several corrections are introduced in the chip design. A new version of the ASIC is ordered and is expected to be ready by the middle of 2019.

References

- [1] K.A. Ten, E.R. Prueel, L.A. Merzhievsky, et al., Tomography of the flow field of detonation product using SR, *Nucl. Instrum. Methods* 603 (2009) 160–163.
- [2] V.M. Titov, E.R. Prueel, K.A. Ten, et al., Experience of using synchrotron radiation for studying detonation processes, *Combust. Explos. Shock Waves* 47 (6) (2011) 615–626.
- [3] E.R. Prueel, K.A. Ten, B.P. Tolochko, et al., Implementation of the capability of synchrotron radiation in a study of detonation processes, *Doklady Phys.* 58 (1) (2013) 24–28.
- [4] K.A. Ten, E.R. Prueel, A.O. Kashkarov, et al., Detection of particle ejection from shock-loaded metals by synchrotron radiation methods, *Combust. Explos. Shock Waves* 54 (5) (2018) 606–613.
- [5] V. Aulchenko Papishev, S. Ponomarev, L. Shekhtman, V. Zhulanov, Development of a one-dimensional detector for the study of explosions with a synchrotron radiation beam, *J. Synchrotron Rad.* (10) (2003) 361–365.
- [6] V. Aulchenko, O. Evdokov, S. Ponomarev, L. Shekhtman, et al., Development of fast one-dimensional X-ray detector for imaging of explosions, *Nucl. Instrum. Methods A* 513 (2003) 388–393.
- [7] V.M. Aulchenko, O.V. Evdokov, L.I. Shekhtman, et al., Detector for imaging of explosions: present status and future prospects with higher energy X-rays, *J. Instrum.* 3 (2008) P05005.
- [8] V.M. Aulchenko, O.V. Evdokov, L.I. Shekhtman, et al., Current status and further improvements of the detector for imaging of explosions, *Nucl. Instrum. Methods. A* 603 (2009) 73–75.
- [9] V.M. Aulchenko, S.E. Baru, O.V. Evdokov, et al., Fast high resolution gaseous detectors for diffraction experiments and imaging at synchrotron radiation beam, *Nucl. Instrum. and Methods. A* 623 (2010) 600–602.
- [10] L.I. Shekhtman, V.M. Aulchenko, A.E. Bondar, A.D. Dolgov, et al., GEM-Based detectors for SR imaging and particle tracking, *J. Instrum.* 7 (2012) C03021.
- [11] L.I. Shekhtman, V.M. Aulchenko, V.N. Kudryavtsev, et al., Upgrade of the detector for imaging of explosions, *Physics Procedia* 84 (2016) 189.
- [12] V. Aulchenko, E. Prueel, L. Shekhtman, et al., Development of the microstrip silicon detector for imaging of fast processes at a synchrotron radiation beam, *Nucl. Instrum. Methods* 845A (2017) 169–172.
- [13] Tolochko B.P., A.V. Kosov, O.V. Evdokov, et al., The synchrotron radiation beamline 8-b at VEPP-4 collider for SAXS, WAXS and micro tomography investigation of fast processes at extreme condition of high temperature and pressure with nanosecond time resolution, *Physics Procedia* 84 (2016) 427.
- [14] G. Baranov Vobly, E. Levichev, et al., Hybrid magnet wiggler for SR research program at VEPP-4M, *Physics Procedia* 84 (2016) 126.
- [15] A. Piminov, G.N. Baranov, A.V. Bogomyagkov, et al., Synchrotron radiation research and application at VEPP-4, *Physics Procedia* 84 (2016) 19.
- [16] <http://www.esrf.eu/Instrumentation/software/data-analysis/xop2.4>.